Novel role of cold/menthol-sensitive transient receptor potential melastatine family member 8 (TRPM8) in the activation of store-operated channels in LNCaP human prostate cancer epithelial cells.

Stephanie Thebault, Loic Lemonnier, Gabriel Bidaux, Matthieu Flourakis, Alexis Bavencoffe, Dimitri Gordienko, Morad Roudbaraki, Philippe Delcourt, Yuri Panchin, Yaroslav Shuba, et al.

NOVEL ROLE OF COLD/MENTHOL-SENSITIVE TRPM8 IN THE ACTIVATION OF STORE-OPERATED CHANNELS IN LNCaP HUMAN PROSTATE CANCER EPITHELIAL CELLS

S. Thebault[†], L. Lemonnier[†], G. Bidaux[†], M. Flourakis, A. Bavencoffe, D. Gordienko[1], M. Roudbaraki, P. Delcourt, Y. Panchin[2], Y. Shuba[‡3], R. Skryma[¶], and N. Prevarskaya[¶]

Laboratoire de Physiologie Cellulaire, INSERM EMI 0228, USTL SN3, 59655 Villeneuve d'Ascq, France

Running title: ER function of TRPM8 channel in LNCaP cells

Address correspondence to: Natalia Prevarskaya, Laboratoire de Physiologie Cellulaire, INSERM EMI 0228, Bâtiment SN3, USTL, 59655 Villeneuve d'Ascq, France; Tel.: 33-3-20-43-4077; Fax: 33-3-20-43-4066; E-mail: Natacha.Prevarskaya@ univ-lille1.fr

Recent cloning of a cold/menthol-sensitive TRPM8 channel (Transient Receptor Potential Melastatine family member 8) from rodent's sensory neurons has provided the molecular basis for the cold sensation. Surprisingly, the human orthologue of rodent's TRPM8 also appears to be strongly expressed in the prostate and the prostate cancer-derived epithelial cell line, LNCaP. In this study we show that, despite such expression, LNCaP cells respond to cold/menthol stimulus by membrane current ($I_{cold/menthol}$), which shows inward rectification and high Ca^{2+} selectivity, which are drastically different properties to the "classical" TRPM8-mediated $I_{cold/menthol}$. Yet, silencing of endogenous TRPM8 mRNA by either antisense or siRNA strategies suppresses both $I_{cold/menthol}$ and TRPM8 protein in LNCaP cells. We demonstrate that these puzzling results arise from TRPM8 localization not in the plasma, but in the endoplasmic reticulum (ER) membrane of LNCaP cells, where it supports cold/menthol/icilin-induced Ca^{2+} release from the ER with concomitant activation of plasma membrane (PM) store-operated channels (SOC). In contrast, GFP-tagged TRPM8 heterologously expressed in HEK-293 cells target the PM. We also demonstrate that TRPM8 expression and the magnitude of SOC current associated with it are androgen-dependent. Our results suggest that the TRPM8 channel may be an important new ER Ca^{2+} release channel, potentially involved in a number of Ca^{2+}- and store-dependent processes in prostate cancer epithelial cells, including such important ones for prostate carcinogenesis as proliferation and apoptosis.

Mammalian homologues of the *Drosophila* TRP (Transient Receptor Potential) channel, which initially emerged as channels specifically linked to phospholipase C (PLC) catalyzed inositol phospholipids breakdown signaling pathways, have now grown into a broad family of channel-forming proteins displaying extraordinarily diverse activation mechanisms (for reviews see (1-5)). At present, these channels are grouped into 6 subfamilies based on structural homology and have received a unified nomenclature (5).

A number of mammalian TRPs show a unique mode of gating, in response to thermal stimuli as well as to the chemical imitators of burning and cooling sensations, capsaicin and menthol, respectively. As such, they represent a group of thermal receptors covering a wide range of physiological temperatures. Most of the thermal receptors belong to the vanilloid TRP subfamily (TRPV, (6)) including warmth-sensitive (<40° C) TRPV3 (7-9), heat- and capsaicin-sensitive TRPV1 (>43° C) (10) and TRPV2 (>52° C) (11). On the other hand, sensitivity to cooling temperatures (<22° C) and menthol is mediated by a structurally distant thermal receptor, TRPM8, belonging to the melastatin (TRPM) subfamily of TRP channels (12, 13), whilst the ankyrin transmembrane protein 1 (ANKTM1 or TRPA1) is involved in the detection of noxious cold (14).

Consistent with their role in the sensation of distinct physiological temperatures, thermal receptors are mostly expressed in subsets of sensory neurons, where they participate in the conversion of various thermal stimuli into an electrochemical form valid for further propagation to the integrative centers of the central nervous system (CNS) as well as to skin cells. Interestingly, the 92% identical human orthologue of a rodent's cold receptor, initially termed as trp-p8 (15), is almost exclusively expressed in the male reproductive system. In fact, testis and prostate tissues were shown to be the only normal human tissues outside the nervous system to express cold receptor TRPM8-related transcripts

(15). Moreover, whilst remaining at moderate levels in a normal prostate, trp-p8 expression greatly increases in prostate cancer. Other non-prostatic primary human tumors of breast, colon, lung and skin also become highly enriched in trp-p8, whereas in the corresponding normal tissues it is virtually undetectable (15). All this suggests that aside from its already established role in cold sensation, TRPM8 is likely to have other important functional roles, especially in the prostate, and during carcinogenesis.

In the present study, we focused on the characterization of the endogenous TRPM8 in the model system of human LNCaP (Lymph Node Carcinoma of the Prostate, (16)) androgen-dependent prostate cancer epithelial cells. We show that LNCaP cells, although expressing TRPM8 transcripts and protein, nevertheless generate a membrane current in response to cold or menthol with drastically different biophysical properties from those initially described for sensory neurons and heterologously expressed TRPM8 (e.g., (12, 13)). In contrast to "classical" TRPM8-mediated current ($I_{cold/menthol}$), which is characterized by outward rectification and poor cationic selectivity (12, 13), menthol-activated current in LNCaP cells shows strong inward rectification and high calcium selectivity; which could nevertheless, still be suppressed by experimental maneuvers which decrease endogenous TRPM8 mRNA and protein expression. We demonstrate that these puzzling results are explained by the exclusive extraplasmalemmal localization of TRPM8 mostly in the endoplasmic reticulum (ER) membrane of LNCaP cells where in response to cold or menthol, it is able to induce the release of calcium ions. Concomitant ER Ca^{2+} store depletion activates Ca^{2+} entry *via* plasma membrane store-operated channels (SOC), which could be detected in electrophysiological experiments as $I_{SOC/menthol}$ with biophysical properties identical to those of the store-operated currents described in our previous works (17-21). In contrast, TRPM8 cloned from human prostate and heterologously expressed in HEK-293 cells shows dual localization in the ER as well as in the plasma membrane (PM), where it mediates "classical" $I_{cold/menthol}$. We also show that TRPM8 expression in LNCaP cells and the associated $I_{SOC/menthol}$ magnitude are androgen-dependent. Our results suggest that TRPM8 may be an important ER Ca^{2+} release channel potentially involved in a number of Ca^{2+}- and store-dependent processes in prostate cancer epithelial cells, including such important ones for prostate carcinogenesis as proliferation and apoptosis.

EXPERIMENTAL PROCEDURES

Cell cultures – LNCaP cells from the American Type Culture Collection were cultured as described previously (17-21). HEK-293 cells were cultured in Dulbecco's minimal essential medium (DMEM) (Gibco-BRL, CergyPontoise, France) supplemented with 10% fetal calf serum and kanamycin (100 µg/ml).

Electrophysiology and solutions – The whole-cell patch-clamp technique was used for membrane currents recording. This technique has been described in detail elsewhere (17-21). The average cell capacitance of LNCaP and HEK-293 (wild-type and TRPM8-expressing) cells were 23.6±1.9 pF and 19.4±1.6 pF, respectively. The composition of the normal extracellular solutions used for electrophysiological recordings was (in mM): 140 NaCl, 5 KCl, 2 $CaCl_2$, 2 $MgCl_2$, 0.3 Na_2HPO_4, 0.4 KH_2PO_4, 4 $NaHCO_3$, 5 glucose, 10 HEPES (pH adjusted to 7.3 with NaOH). Extracellular solution used to record Ca^{2+}-carried $I_{SOC/menthol}$ contained (in mM): 150 N-Methyl-D-Glucamine (NMDG), 10 $CaCl_2$, 10 HEPES (pH adjusted to 7.3 with HCl). The changes in external solutions were carried out using a multi-barrel puffing micropipette with a common outflow, positioned in close proximity to the cell under investigation. During the experiment, the cell was continuously superfused with the solution via a puffing pipette to reduce the possibility of artifacts occuring due to the switch from a static to a moving solution and vice versa. Complete external solution exchange was achieved in <1 s. Intracellular pipette solution used to record $I_{SOC/menthol}$ in LNCaP cells contained (in mM): 100 NMDG, 20 NaCl, 10 HEPES, 8 EGTA, 3.1 $CaCl_2$, 1 $MgCl_2$ (pH adjusted to 7.3 with HCl). Otherwise we used K^+- or Cs^+-based intracellular solutions (in mM): 100 KOH (CsOH), 40 KCl (CsCl), 5 HEPES, 8 EGTA, 3.1 $CaCl_2$, 1 $MgCl_2$ (pH adjusted to 7.3 with glutamic acid). The free concentrations of divalent cations in the solution

containing a chelating agent, were estimated using WinMaxc 1.7 software (22). All chemicals were obtained from Sigma (Sigma-Aldrich, Steinheim, Germany). For all Ca^{2+} imaging and electrophysiological experiments, the temperature of the cell bath solution was adjusted to 36°C, unless otherwise specified.

Cloning of trpm8 cDNA and fusion protein construction – *Trpm8* gene from normal human prostate was cloned from 1 µg of Human prostate polyA+ RNA (Clontech, Palo Alto, USA) by SMART PCR cDNA synthesis Kit (Clontech). Primers for TRPM8 amplification were: 5'-ACCAGCTAGCATGTCCTTTCGGGCAGCCGG GCTC-3' (forward) and 5'-AGATCTCGAGTTTGATTTTATTAGCAATCT CTTTCA-3' (backward). PCR was performed by Advantage-HF PCR Kit (Clontech). The PCR product was purified by a MinElute PCR Purification Kit (QIAGEN) and digested with XhoI (NEB). pEGFP-N1 plasmid DNAs (Clontech) were linearized with NheI (NEB) and blunt ends were generated by DNA Polymerase I Klenow Fragment (NEB). After DNA purification by phenol/chloroform extraction, the vectors were again digested with XhoI and phenol/chloroform extracted. The digested PCR product was ligated into the vectors and recombinant clones were selected by PCR.

Trpm8 gene from LNCaP cells was cloned from 4 µg of total mRNA. Reverse transcription was performed using SuperScript™ III Reverse Transcriptase (Invitrogen Inc, Cergy Pontoise, France) and Random Hexamer Oligonucleotides (Perkin Elmer) following the manufacturers instructions. PCR was performed using the forward primer: 5'-CCTGCTTGACAAA AACCGTC-3' and backward primer: 5'-TCTCAAGGTCTCAGCACACTA-3', BD Advantage™ 2 PCR enzyme system (Clontech). PCR products were analyzed on agarose, and a band of about 3.5 kbp was cloned into pcR2.1 vector with a TOPO® TA cloning kit (Invitrogen Inc). After sequencing, the plasmid was digested by EcoRI (NEB) and the two restricted fragments were ligated into a pcDNA4 vector (Invitrogen) which had previously been digested by EcoRI. Restriction analysis of positive clones was then done to detect correct *trpm8* gene insertion.

RT-PCR analysis of TRPM8 expression – Total RNAs were isolated from several cell lines: LNCaP, DU-145, PC-3, PNT1A and HEK-293 cells as described elsewhere (31). After a DNase I treatment (Invitrogen), 2.5 µg of total RNA were reverse transcribed and followed by PCR, as described. The PCR primers (Invitrogen) used to amplify the RT-generated TRPM8 were 5' GAT TTT CAC CAA TGA CCG CCG 3' (forward) and 5' CCC CAG CAG CAT TGA TGT CG 3' (backward). To detect TRPM8 cDNAs, PCR was performed by adding 2 µl of the RT template to a mixture of (final concentrations): 50 mM KCl, 10 mM Tris-HCl (pH 8.3), 2.5 mM $MgCl_2$, 200 µM of each dNTP, and 1 U AmpliTaq Gold (Applied Biosystems) in a final volume of 25 µl. DNA amplification conditions included an initial denaturation step of 7 min at 95°C, and 40 cycles of 30 s at 95°C, 30 s at 60°C, 40 sec at 72°C, and finally 7 min at 72°C.

Transient transfection – HEK-293 cells were cultured in 35 mm diameter Petri dishes for cell recordings (Nunc) until 50-60% of confluency. Then cells were transiently transfected by either 2 µg (in 35 mm dishes) of plasmid (transfecting either pEGFP/TRPM8-N1, or pcDNA4/TRPM8 plus pEGFP-N1 at 5:1 ratio, or pEGFP-N1 alone) using a Gene Porter™2 Transfection Reagent (Gene Therapy Systems, Inc. (GTS) San Diego) following the manufacturers instructions.

Creation of HEK-293 cell line stably expressing TRPM8 – Tetracycline repressor-expressing HEK-293 cells (Invitrogen) were transfected with 2 µg of a TRPM8-pcDNA4.TO. vector as describe before. 3 days after transfection cells were submitted to Zeocin selection (500 µg/ml) for 10 days. 8 positive clones were isolated and checked for the tetracycline-induction of full-size TRPM8 channel expression and function and all of them appeared to be equivalent. Therefore, no distinction among clones was made in the functional studies.

siRNA cell transfection – LNCaP cells were transfected overnight with 100 nM $siRNA_{TRPM8}$, using either 5 µl or 15 µl of TransIT-TKO transfection reagent (Mirus Inc, Madison, USA) following the manufacturers instructions. All experimentations were carried out 48 hours after transfection.

Ready-to-use siRNA (processing option: A4) was synthesized by Dharmacon Inc (Lafayette, USA). The sense sequence of

$siRNA_{TRPM8}$ was: 5'-TCTCTGAGCGCACT ATTCA(dTdT)-3' (position 894-912 on TRPM8 sequence, accession number: NM_024080.3). Control siRNA experiments were performed either by applying the transfection reagent alone (vehicle) or by transfecting a specific siRNA against Pannexin 1 protein ($siRNA_{Pan}$) 5'-ACGATTTGAGCCTCTACAA(dTdT)-3' (position 1361-1379 on Pannexin 1 sequence, accession number: NM_015368). Neither vehicle nor control vector influenced the expression of both TRPM8 mRNAs and proteins.

Immunohistochemistry – 60% confluent LNCaP cells were fixed with 4% formaldehyde-1X PBS for 15 minutes. After three washs the cells were either incubated in FITC-conjugated Cholera toxin subunit B ("CTB", C-1655, SIGMA-Aldrich, dilution: 1/2000) diluted in 1X PBS at room temperature for 20 minutes and then washed three times before to be permeabilize or were directly permeabilized in PBS-gelatine (Phosphate buffer saline, gelatine 1.2%) complemented with 0,01% Tween 20 and 100mM glycin for 30 minutes at 37°C. Afterwards the cells were co-incubated with a primary rabbit polyclonal anti-TRPM8 antibody (code: ab3243, Abcam, Cambridge, UK) diluted (1/200) in PBS-gelatine for 1 hour at 37°C. After thorough washes in PBS-gelatine, the slides were treated with the corresponding Alexa fluor 546-labeled anti-rabbit IgG (A-21206, Molecular probes, used dilution: 1/4000) diluted in PBS-gelatine for 1 hour at room temperature. After two washes in PBS-gelatine and one in PBS, the slides were mounted with Mowiol®.

Fluorescence analysis was carried out using a Zeiss LSM 510 confocal microscope (488 nm excitation for FITC and 546 nm for Alexa-546) connected to a Zeiss Axiovert 200 M with a 40X1.3 numerical aperture oil immersion objective. Both channels were excited, collected separately and then merged to examine colocalization. The image acquisition characteristics (pinhole aperture, laser intensity, etc.) were the same throughout the experiments to ensure the comparability of the results. Using confocal microscope software (AIM 3.2, Zeiss, Le Pecq, France), the colocalization coefficients were calculated in the manner defined by Manders *et al.* (24).

For the immunofluorescence quantification of TRPM8 expression in LNCaP cells transfected with either control or anti-TRPM8 siRNAs, all confocal images were acquired under standard conditions (pinhole aperture, laser intensity, etc.) and analyzed using confocal microscope software (AIM 3.2, Zeiss, Le Pecq, France) to determine the specific mean cell intensity for each experiment and then to calculate the average and standard deviation for four independent areas.

Western-blot assay – Total protein fraction from the cells of interest was harvested in PBS and then sonicated in an ice-cold buffer (pH 7.2) containing (in mM): 20 HEPES, 50 NaCl, 10 EDTA, 1 EGTA, 1 PMSF, 1% NP40, a mixture of protease inhibitors (Sigma, L'Isle d'Abeau Chesnes, France), and a phosphatase inhibitor (sodium orthovanadate, Sigma). Samples (40 µg each) were electrophoretically analyzed on 10% polyacrylamide gel using the SDS-PAGE technique. The proteins were then transferred for 1.5 hours (50 mA, 25 V) onto a nitrocellulose membrane using a semi-dry electroblotter (Bio-Rad). The membrane was blocked in 5% TNT-milk (15 mM Tris buffer pH 7.4, 140 mM NaCl, 0.05% Tween 20 and 5% non-fat dry milk) for 30 minutes at room temperature, then soaked overnight at +4°C either in a 1/500 diluted primary rabbit polyclonal anti-TRPM8 antibody (code: ab3243, Abcam, Cambridge, UK), or in a 1/500 primary rabbit polyclonal anti-actin (Neomarkers, MS-1295-P) both diluted in 3% TNT-milk. After three 15-min washes in TNT, the membrane was transferred into anti-rabbit-IGg horseradish peroxidase-linked secondary antibodies (Chemicon, USA), diluted in 3% TNT-milk (1/20000) for 1 hour. After three 10-min washes in TNT, the membrane was processed for chemiluminescent detection using Supersignal West Pico chemiluminescent substrate (Pierce, Chemical Company, Rockford, IL), according to the manufacturer's instructions. The blots were then exposed to X-Omat AR films (Eastman Kodak Company, Rochester, NY).

Ca^{2+} imaging – Cytosolic Ca^{2+} concentration ($[Ca^{2+}]_c$) was measured using ratiometric dye Fura-2 and quantified according to Grynkiewicz and Tsien formula (25). For confocal $[Ca^{2+}]_c$ imaging, cells were loaded with non-ratiometric Fluo-3AM dye. During measurements, the cells were bathed in the same normal extracellular solution as used for electrophysiological recording. To produce Ca^{2+}-

free conditions, $CaCl_2$ was removed from this solution and EGTA (0.5 mM) was added. For Ca^{2+} imaging within the ER, LNCaP, cells were grown on glass coverslips and loaded with 5 μM of Mag-Fluo-4AM (Molecular Probes, Leiden, The Netherlands), for 45 min at 37°C. After incubation with the dye, the plasma membrane was selectively permeabilized: cells were rinsed briefly in a high-K^+ solution of the following composition (in mM): 125 KCl, 25 NaCl, HEPES, 10; EGTA, 1; $CaCl_2$, 0.5; $MgCl_2$, 0.1 (free Ca^{2+} clamped to 170 nM, pH 7.2), and exposed for 1 min to the same solution at 37°C in the presence of digitonin (0.5 mg/ml). Permeabilized cells were then continuously perfused with the high K^+ solution supplemented with 0.2 mM Mg-ATP. Confocal imaging was performed using a Zeiss LSM 510 confocal microscope.

Data analysis **–** The data were analyzed using PulseFit (HEKA Electronics, Germany) and Origin 5.0 (Microcal Software Inc., Northampton, MA, USA). Results were expressed as mean ± standard error of the mean (s.e.m.). Statistical analysis was performed using the student's *t*-test ($P<0.05$ considered significant) and ANOVA tests followed by Tukey-Kramer post-tests.

RESULTS

Expression of the full-length TRPM8 in LNCaP cells **–** Although previous studies have shown the expression of TRPM8 transcripts (15, 26) and even protein labeling (26) in LNCaP cells, to be a necessary prerequisite for functional studies, we first sought to confirm endogenous TRPM8 mRNA expression in these cells by RT-PCR and to compare that to other cell lines of prostatic origin. Fig. 1A shows that out of four prostatic cell lines tested, namely the normal prostate epithelial cell line PNT1A, the androgen-dependent prostate cancer epithelial cell line LNCaP and androgen-independent prostate cancer epithelial cell lines DU145 and PC3, only in LNCaP cells could the TRPM8 mRNA-specific amplification fragment be detected. No such fragment was evident in the most popular heterologous expression system, namely wild-type HEK-293 cells.

Given that expression of endogenous full-length TRPM8 transcript has never been demonstrated in LNCaP cells, and the degree of its homology to human TRPM8 is not known, we isolated the 3312 bp open reading frame of the full-length TRPM8 cDNAs from both LNCaP cells and human prostate (see Experimental Procedures for details). Sequencing of both clones showed quite perfect homology between them (99,97 %) and to other published human sequences. Analysis of all TRPM8 clones available from GeneBank revealed two sites of possible single nucleotide polymorphism (SNP) at positions: 173 (T↔C) and 2383 (A↔G) (see Table 1). Thus, from a molecular perspective, endogenous TRPM8 in LNCaP cells is basically identical to the TRPM8 expressed in native human prostate.

Transfection of HEK-293 cells with a pEGFP vector containing a TRPM8 cDNAinsert (which we cloned from human prostate, GeneBank: AY328400; HEK-293/pEGFP-TRPM8 cells) resulted in the appearance of TRPM8 mRNA-specific amplification fragments detected by RT-PCR, whereas in both the wild-type (HEK-293/wt) and the empty vector transfected (HEK-293/pEGFP) HEK-293 cells, no such fragment could be detected (Fig. 1B).

Using pEGFP-TRPM8 plasmid for HEK-293 cell transfection directs the expression of the fusion construct, in which GFP is attached to the TRPM8 C-terminus. Such a construct is advantageous when studying the subcellular distribution of heterologously expressed TRPM8 based on GFP fluorescence. However, the influence of GFP on TRPM8 functional properties cannot be excluded. Therefore, for functional studies of recombinant TRPM8 we also used HEK-293 cells transiently co-transfected with separate pcDNA4 plasmid containing TRPM8 cDNA insert and pEGFP plasmid (HEK-293/pcDNA4-TRPM8+pEGFP cells), as well as an HEK-293 cell line newly created in our laboratory, stably expressing TRPM8 under tetracycline-inducible promoter (HEK-293/TRPM8 cells). The same cells, but without tetracycline induction were used for control purposes (HEK-293/ctrl cells), since RT-PCR detection of TRPM8 expression in such cells was negative (data not shown). Our control experiments did not reveal any notable differences in the protein targeting, menthol-sensitivity and voltage-dependence of TRPM8-carried currents in HEK-293/pEGFP-TRPM8,

HEK-293/pcDNA4-TRPM8+pEGFP or HEK-293/TRPM8 cells.

LNCaP cells and TRPM8-expressing HEK-293 cells exhibit distinct functional responses to menthol – Functional responses to temperature decrease or menthol exposure, which are the interventions known to activate endogenous and heterologously expressed TRPM8 (12, 13) were investigated using a patch-clamp technique for activation of membrane currents.

Both endogenous $I_{cold/menthol}$ in sensory neurons and the current associated with heterologous expression of rodent's TRPM8 were shown to be outwardly rectifying and mainly carried by monovalent cations (12, 13). Consistent with these findings, TRPM8-expressing HEK-293 cells responded to menthol application (100 μM) by generating an outwardly rectifying current ($I_{menthol}$), which was absent in the ctrl/HEK-293 cells (Fig. 2A). In contrast, application of menthol to the whole-cell patch-clamped LNCaP cells under physiological ionic conditions from both sides of the membrane (i.e., K^+- and Na^+-based intra- and extracellular solutions, respectively; see Experimental Procedures) failed to evoke any notable outward current on top of the voltage-dependent K^+ one inherent to LNCaP cells (Fig. 2B, n=6) described in our previous works (27, 28). It should be noted that the superficially endogenous K^+ current in LNCaP cells is similar to the TRPM8-mediated $I_{menthol}$ – both being outwardly rectifying. Thus, in the event of plasmalemmal TRPM8 expression, one would expect a menthol-induced enhancement of the outward current. Instead, at higher resolutions, we were even able to detect the appearance of some small inward currents in response to menthol in LNCaP cells (Fig. 2B, inset).

The lack of "classical" TRPM8-mediated $I_{menthol}$ in LNCaP cells seems to be in conflict with the robust TRPM8 mRNA expression detected by RT-PCR (see Fig. 1A). This controversy can be explained by either predominant non-plasmalemmal localization of the mature TRPM8 protein or by specific post-translational processing resulting in the loss of functional properties. To investigate subcellular TRPM8 distribution we used two strategies. First, we transfected LNCaP cells with GFP-tagged recombinant TRPM8 and examined the targeting of heterologously expressed construct based on GFP fluorescence Second, we used fluorescent-labeled anti-TRPM8 antibody to visualize endogenously expressed protein.

Fig. 2C compares representative confocal images of HEK-293 cells (left panel) and LNCaP cells (right panel) heterologously expressing GFP-tagged TRPM8. Inspection of both images shows substantial GFP fluorescence associated with intracellular compartments in both cell types. However, if in HEK-293 cells clear clusters of GFP fluorescence are also evident on the cell's perimeter, then in LNCaP cells such peripheral fluorescence was completely lacking. Such patterns of GFP fluorescence are consistent with combined intracellular and plasmalemmal localization of chimera TRPM8/GFP protein in HEK-293 cells, but only intracellular localization in LNCaP cells. Furthermore, a bright fluorescence was detectable in perinuclear membranes of both cell lines. Accordingly to the differencies in TRPM8/GFP localization, we were unable to detect any "classical" $I_{menthol}$ either in the regular LNCaP cells (i.e., Fig. 2B), or following heterologous expression of TRPM8/GFP construct (data not shown), whereas in HEK-293/pEGFP-TRPM8 cells "classical" $I_{menthol}$ could be readily activated (i.e., Fig. 2A).

To verify the subcellular localization of endogenous TRPM8 protein in LNCaP cells, we utilized double staining with specific anti-TRPM8 antibody and FITC-conjugated Cholera toxin subunit B (CTB). The latter specifically interacts with GM1 lipids and therefore serves as a plasma membrane marker (29, 30). As shown in Fig. 2D, green fluorescence of CTB is strictly limited to the PM (middle panel), whereas red-detection of TRPM8 appears to be mostly dotted in the cell body (left panel). Overlay of the two images (right panel) did not reveal any yellow color, which would be indicative of TRPM8 and CTB co-localization, and thus provide evidence of TRPM8 location in the plasma membrane. This observation was quantitatively confirmed by the calculation of the co-localization coefficients (24) in 10 different PM-including regions of interest (ROI) belonging to 8 different cells, as exemplified in the right panel of Fig. 2D (ROI is encompassed by the thin light blue line). The CTP/TRPM8 co-localization coefficient averaged at only 3±2%, indicating that only an insignificant proportion of TRPM8 proteins (i.e., 3±2%) is located with in the PM. It

is important to note that, due to the optical limitations of a confocal microscope, a protein should be considered to have essential plasma membrane localization when the co-localization coefficient with PM marker exceeds 10% and is at least significantly different from 0.

Interestingly, the immunodetection of TRPM8 did not reveal any strong perinuclear localization if compared with that we detected for TRPM8/GFP overexpression. However, we do not exclude that several TRPM8 proteins might be present into the perinuclear membrane; we likely assume that the TRPM8 overexpression either produced an artifact of localization or drastically overinduced a normaly weak translocation to this membrane.

Thus when taken together, our data suggest that neither endogenous nor heterologously expressed TRPM8 channels are targeted at the plasma membrane of LNCaP cells, which we believe is the primary reason for the lack of "classical" $I_{menthol}$ in this particular type of prostate cancer epithelial cells.

TRPM8 mediates qualitatively different cold/menthol responses in LNCaP cells – Recently, it has been suggested that TRPM8 is present in the ER membrane of LNCaP cells, where it may function as cold/menthol-sensitive Ca^{2+} release channel (26). Our data showing exclusive TRPM8 targeting of intracellular compartment(s) of LNCaP cells support the idea of such a functional role. If this is in fact the case, then TRPM8-mediated Ca^{2+} release from the ER in response to cold/menthol should activate store-operated plasma membrane channels (SOC), which can be detected as store-operated Ca^{2+} current (I_{SOC}) in patch-clamp experiments. Our observation that exposure of LNCaP cells to menthol elicits not "classical" outwardly rectifying $I_{menthol}$, but rather a small inward current (see Fig. 2B, inset) is consistent with such expectations. Moreover, the fact that this current was sensitive to the extracellular Ca^{2+} removal (data not shown), suggested that Ca^{2+} is a major charge carrier, which is typical of highly Ca^{2+}-selective SOCs in LNCaP cells (17-21).

In order to better resolve menthol-activated current in LNCaP cells, we formulated intra- and extracellular solutions, which allowed the elimination of voltage-dependent K^+ and the minimization of other possible currents (due to K^+, Na^+ replacement with impermeable NMDG; see Experimental Procedures) and raised the extracellular Ca^{2+} concentration ($[Ca^{2+}]_{out}$), as a potential charge carrier, to 10 mM. Under such conditions, both cold stimulus (a temperature drop from 36° to 22° C, Fig. 3A) and menthol (100 μM, Fig. 3B) activated membrane currents with prominent inward rectification. These currents were indeed quite small at –100 mV averaging at only 1.13 ± 0.36 pA/pF (n=6) and 1.24 ± 0.37 pA/pF (n=5) for cold and menthol, respectively (Fig. 3A, B, compare to ~60 pA/pF for voltage-dependent K^+ current, Fig. 2B), had very positive reversal potential (around +50 mV, inset of Fig. 3A, B), and disappeared upon extracellular Ca^{2+} removal (data not shown), as is consistent with the activation of plasma membrane Ca^{2+}-permeable cationic channels in LNCaP cells.

Cationic selectivity of menthol-activated channels in LNCaP cells was characterized by measuring current amplitudes (at –100 mV) following equimolar substitutions of Ba^{2+}, Sr^{2+}, Mn^{2+}, Na^+ or K^+ for 10 mM Ca^{2+} in the extracellular saline and relating them to the amplitude of the Ca^{2+} current. A summary of the selectivity measurements for 4-to-6 of each ion substitutions is presented in Fig. 3C. Maximal currents carried by tested ions can be placed in the following order: $Ca^{2+}(1) > Ba^{2+}(0.40 \pm 0.10) \sim Sr^{2+}(0.39 \pm 0.03) > Mn^{2+}(0.16 \pm 0.14) > Na^+(0.12 \pm 0.04) > K^+(0.06 \pm 0.07)$. This order appears to be very similar to the one found for endogenous SOCs in LNCaP cells (19, 20).

In addition, menthol-activated Ca^{2+} current in LNCaP cells was inhibited by such common inhibitors of native cationic channels and heterologously expressed TRP members such as ruthenium red (10 μM, n=4), SK&F 96365 (50 μM, n=6) and flufenamate (10 μM, n=5). The results of the respective experiments are summarized in Fig. 3D. All agents produced fast and reversible current inhibition, which was comparable in size to their effects on I_{SOC}, as known from our previous works (19, 20).

Altogether, our patch-clamp experiments unequivocally demonstrate remarkable similarity of principal biophysical properties of menthol-activated and store-operated currents in LNCaP cells. Such a similarity strongly suggests that both currents are likely to be carried by the same

system of plasma membrane store-dependent cationic channels. In order to highlight two distinguishing features: menthol as an initial activating stimulus and SOCs as the transmembrane pathway involved, we propose to call the menthol-activated current in LNCaP cells $I_{SOC/menthol}$.

TRPM8 acts as an ER Ca^{2+} release channel in the $I_{SOC/menthol}$ activation pathway – Our working hypothesis was that application of menthol activates TRPM8, localized in the ER membrane of LNCaP cells, which produces ER Ca^{2+} store depletion followed by the activation of plasma membrane SOCs, detected in the form of $I_{SOC/menthol}$ in electrophysiological experiments. To specifically prove the role of TRPM8 in this pathway, we utilized the strategy of knocking down TRPM8 mRNA either by means of antisense oligodeoxynucleotides (ODNs) or by siRNA, with a subsequent evaluation of what impact this may have on functional responses.

In the series of TRPM8 hybrid depletion experiments, we used LNCaP cells treated for 60 hours with TRPM8-specific antisense ODNs (see Experimental Procedures). The cells treated for the same period of time with respective sense ODNs, which are not supposed to alter endogenous TRPM8 expression, served as a control. Western blot analysis with TRPM8-specific antibody (see Experimental Procedures) confirmed a significant reduction in TRPM8 protein in antisense- vs. sense-treated cells (Fig. 4A). Surprisingly, Western blot analysis of LNCaP and HEK-293/TRPM8 cells produced a number of specific bands. We assume that, with the exception of the 125 kDa band which corresponds to the normal TRPM8, the more intense band observed in both cell types may represent TRPM8 dimer (about 250 kDa), whilst smaller bands of about 50 and 75 kDa might represent cleavage products of the normal TRPM8. Furthermore, LNCaP cells exhibited an additional intermediate triplet of about 95 kDa, which was not observed in HEK-293/TRPM8, but which could be specifically silenced by antisense treatment. It may well be that this triplet represents a new TRPM8 isoform.

As documented in Fig. 4B, $I_{SOC/menthol}$ density (measured at –100 mV) following antisense treatment was about 72% lower than the control (i.e., from –0.81±0.18 pA/pF, n=6 to –0.14±0.06 pA/pF, n=8), suggesting a direct correlation between endogenous TRPM8 expression and $I_{SOC/menthol}$ magnitude.

Qualitatively and quantitatively similar results were obtained using siRNA technology to downregulate endogenous TRPM8 expression in LNCaP cells. Fig. 4D (upper panel) presents the dynamics of TRPM8 mRNA changes assayed by semi-quantitative RT-PCR on the 2^{nd}, 4^{th} and 7^{th} day after transfection with 100 nM of $siRNA_{TRPM8}$. This enabled an estimation of TRPM8 mRNA reduction at these periods of 99±2%, 65±10% and 10±5%, respectively. Immuno-staining with anti-TRPM8 antibody on the 2^{nd} day after transfection followed by semi-quantitative analysis of confocal images (Fig. 4D, lower panel) demonstrated that the level of TRPM8 protein lagged somewhat behind, decreasing by only 83±3% (n=4) compared to control, yet still indicating the effectiveness of the adopted strategy in downregulating endogenous TRPM8 expression. Substantial downregulation of TRPM8 protein in response to $siRNA_{TRPM8}$ treatment was also confirmed by Western blotting (Fig. 4A). As documented in Fig. 4E, such a downregulation was paralleled by about a 42% decrease in maximal $I_{SOC/menthol}$ density at –100 mV (from control –1.24 ± 0.43 pA/pF, n=5 to 0.72 ± 0.27 pA/pF, n=8), further supporting the notion of the involvement of TRPM8 in the pathway leading to $I_{SOC/menthol}$ activation.

In order to directly demonstrate that the role of TRPM8 in this pathway specifically related to the mediation of Ca^{2+} release from the ER in response to menthol, we performed a series of experiments with fluorimetric $[Ca^{2+}]_c$ measurements in LNCaP cells subjected to TRPM8 knock-down by either antisense ODNs or siRNA technology. In this series of experiments, LNCaP cells treated with sense ODNs or a vehicle, served as respective controls.

Figs. 4C and F show that when control LNCaP cells were exposed to menthol (100 µM) in the absence of extracellular Ca^{2+}, this caused a transient $[Ca^{2+}]_c$ elevation, obviously due to Ca^{2+} release from the ER, whereas reintroduction of Ca^{2+} in the continuing presence of menthol produced a rapid $[Ca^{2+}]_c$ elevation due to the initiation of store-operated Ca^{2+} entry (open symbols of Fig. 4C and F, n=72 and 69, respectively). Moreover, as one would expect in the framework of our working hypothesis, TRPM8

knock-down, independently of the strategy employed, abolished both menthol-induced responses,that associated with Ca^{2+} release and that Ca^{2+} entry (filled symbols of Fig. 4C and F, n=64 and 83, respectively). These results can only be explained if TRPM8 operates as a cold/menthol-sensitive ER Ca^{2+} release channel in LNCaP cells.

The ability of menthol to produce TRPM8-mediated ER store depletion was further validated by directly monitoring the Ca^{2+} content of the ER lumen ($[Ca^{2+}]_{ER}$) using compartmentalized fluorescent Ca^{2+} dye Mag-Fluo 4 AM on digitonin-permeabilized LNCaP cells. This technology has been successfully used in our previous studies (18). Fig. 5A documents that application of menthol (100 µM) does indeed produce a 23±3% (n=23) decrease in $[Ca^{2+}]_{ER}$, whereas subsequently applying a saturated concentration of ionomycin (IM, 1 µM, to check for the functionality of stores), depleted the ER store by another 40% (to total 65%). Menthol's ability to lower $[Ca^{2+}]_{ER}$ was not compromised by the combined action of the IP_3 receptor (IP_3-R) blocker heparin (500 µg/ml) and the ryanodine receptor (RyR) blocker ryanodine (20 µM) (Fig. 5B), thereby suggesting the non-involvement of these Ca^{2+} release channels in menthol effects. On the contrary, LNCaP cell treatment with TRPM8 antisense ODNs reduced the ER-depleting action of menthol by almost two-fold (from 20±2%, n=12 in control to 8±2%, n=11, Fig. 5C), highlighting the significant role of TRPM8.

The specificity of the ER depletion to the ER-localized TRPM8 received additional strong support from the experiments on confocal imaging of cytosolic Ca^{2+} in response to another TRPM8 agonist, the super-cooling agent icilin (12). Fig. 6 shows that exposure to icilin (20 µM) caused a strong elevation of $[Ca^{2+}]_c$ in LNCaP cells. The fact that reversible SERCA pump inhibitor cyclopiazonic acid (CPA, 20 µM) did not produce much of an additional $[Ca^{2+}]_c$ rise on top of the icilin-induced one (Fig. 6A), together with the preservation of icilin effects in the absence of extracellular Ca^{2+} (Fig. 6B), indicated icilin action via releasing Ca^{2+} from the ER. Icilin-induced Ca^{2+} release was not impaired by the IP_3-R and RyR blockers xestospongin C (10 µM) and ryanodine (50 µM), respectively, thus confirming its mediation by the ER-localized TRPM8, without any IP_3-R or RyR involvement.

Therefore taken collectively, the results on cytosolic and ER luminal Ca^{2+} measurements unequivocally demonstrated that the TRPM8 agonists, menthol and icilin, indeed act as an ER Ca^{2+} store-depleting agent via ER-localized TRPM8, and that this depletion is sufficient for SOCE activation.

The mode of store-to-SOC coupling involved in menthol effects in LNCaP cells – In our previous study we have shown the existence of two types of SOCs in LNCaP cells with different coupling mechanisms to the ER Ca^{2+} stores. The first type, termed SOC_{CC} (for conformational coupling), relies on direct conformational coupling with an IP_3 receptor (IP_3R) for activation, and the second type, termed SOC_{CIF}, requires the release of a diffusible calcium influx factor (CIF) (21). SOC_{CC}, which carries $I_{SOC/CC}$, is preferentially activated during IP_3-induced store depletion, whereas activation of SOC_{CIF} that carries $I_{SOC/SIF}$ occurs in response to thapsigargin(TG)-mediated store depletion. So, we then asked with what type of SOCs and store-to-SOC coupling mechanism menthol/TRPM8-mediated store depletion interferes most. To answer this question, we utilized combined IP_3/menthol and TG/menthol interventions to check for the additivity of the effects. Fig. 7A shows that activation of $I_{SOC/CC}$ by intracellular infusion of IP_3 (100 µM) plus BAPTA (10 mM) via patch pipette, which recruits IP_3R/SOC conformational coupling mechanism, did not prevent the activation of the full-size $I_{SOC/menthol}$ in response to menthol application. In contrast, the presence of TG (0.1 µM) in the bath solution, which resulted in permanent store depletion, totally abolished the ability of menthol to activate a membrane current (Fig. 7B, n=5). Thus, these results suggest, on the one hand, that menthol and TRPM8 do not interfere with direct IP_3/SOC conformational coupling and, on the other hand, that menthol and TG use common mechanisms, which are presumably CIF-mediated and probably also use a common plasma membrane SOCs for current activation.

TRPM8 expression and function is androgen-dependent – Recently it has been shown by several groups including ours, that TRPM8 expression is androgen-dependent (26, 31). Thus, in view of our present findings on TRPM8 involvement in store-operated Ca^{2+} influx, we

were wondered whether or not the androgen status of prostatic cells has any impact on menthol-activated current. Fig. 8A shows that steroid deprivation using charcoal-stripped culture medium, caused pronounced downregulation of TRPM8 mRNA, as assessed by semi-quantitative RT-PCR, whereas a subsequent addition 5α-dihydrotestosterone (DHT, 10^{-9} M) caused rapid restoration of TRPM8 mRNA and even its further increase above the control levels. The deviations in TRPM8 mRNA expression were paralleled by the changes in $I_{SOC/menthol}$. As Fig. 8B illustrates, exposure to menthol activated about 4-fold smaller $I_{SOC/menthol}$ in LNCaP cells cultured for 96 hours in steroid deprived medium compared to control cells and, as expected, subsequent addition of DHT (10^{-9} M) completely restored $I_{SOC/menthol}$. These variations of $I_{SOC/menthol}$ in response to both steroid deprivation and DHT supplementation basically coincided with the degrees of reduction and restoration of TRPM8 mRNA expression during respective periods (see Fig. 8A). Besides, as demonstrated in Fig. 8C, steroid deprivation prevents both menthol-induced Ca^{2+} release and subsequent store-operated Ca^{2+} entry again confirming our conclusion that $I_{SOC/menthol}$ develops due to the ER store depletion via TRPM8.

DISCUSSION

In the present study we report on four major findings: 1) LNCaP prostate cancer epithelial cells express cold/menthol-sensitive TRPM8, 2) the functional response to cold/menthol involves TRPM8, yet properties of the membrane current are drastically different to the "classical" TRPM8-mediated current, 3) TRPM8 is preferentially expressed in the ER membrane of LNCaP cells, where it plays the role of a cold/menthol-sensitive ER Ca^{2+} release channel, 4) cold/menthol-activated, TRPM8-mediated ER Ca^{2+} store depletion is capable of activating store-operated Ca^{2+} current in LNCaP cells, 5) TRPM8-mediated ER Ca^{2+} store depletion is tightly regulated by androgens.

Molecular properties of human TRPM8 – The analysis of all published TRPM8 sequences revealed two possible single nucleotide polymorphisms at positions 173 (T↔C) and 2383 (A↔G) (see Table 1). We believe, however, that these two mutations are unlikely to account for the lack of TRPM8 plasma membrane expression and/or notable change in its functional properties. Indeed, both the rat and mice TRPM8 sequences (173C, 2383A) were shown to have clear plasma membrane functions (12, 13). Furthermore, we detected plasmalemmal localization and expected "classical" TRPM8-mediated current in HEK-293 cells heterologously expressing human TRPM8 clone with 173C, 2383G polymorphisms. Therefore, the lack of plasma membrane targeting of endogenous TRPM8 in LNCaP cells, which in 173 and 2383 positions coincides with the rodent isoform (i.e., 173C, 2383A), is most likely to be related to the specifics of the post-translational processing of this protein and/or its interactions with some other factor(s), which take place in this type of prostate cancer epithelial cells. Such a conclusion is supported by the fact that heterologously expressed human TRPM8 does not target the PM of LNCaP cells either, although it shows clear PM targeting and function in HEK-293 cells.

It should be noted that in the recent study by Zhang and Barritt (26), TRPM8 was detected in both the ER membrane and plasma membrane of LNCaP cells. The reason for such a discrepancy with our results is not clear, but may be related to the clonal variations of cell line.

Molecular basis of cold/menthol response in LNCaP cells – The apparent similarity of fundamental biophysical properties of $I_{menthol}$ and I_{SOC} (inward rectification and divalent cation selectivity) prompted us to conclude that $I_{menthol}$ is carried through the system of store-operated channels in LNCaP cells and, therefore, could be termed $I_{SOC/menthol}$. This can only be the case if TRPM8 in LNCaP cells acts as a cold/menthol-sensitive ER Ca^{2+} release channel, and activation of $I_{SOC/menthol}$ through the system of plasma membrane SOCs is secondary to menthol-mediated ER store depletion. The bulk of our data, which prove: 1) exclusive TRPM8 localization in the ER membrane of LNCaP cells, 2) the existence of menthol-evoked ER store depletion, 2) concomitant activation of SOCE and 3) the inability of menthol to produce its effects following store depletion by TG, fully agrees with such a possibility. $I_{SOC/menthol}$ activation secondary to menthol-mediated store depletion is also consistent with the slower kinetics of current

activation in LNCaP cells compared to neuronal PM-localized CMR/TRPM8, which are directly gated by menthol.

Localization of TRPM8 on presynaptic Ca^{2+} stores was also suggested for DRG neurons (32). It was concluded that menthol-induced Ca^{2+} release might underlie synaptic transmission facilitation at sensory synapses by menthol. Thus, even in single cell types, such as DRG neuron, TRPM8 may play a dual role, both in cold stimulus perceptions and in the facilitation of synaptic transmission, and such a role is determined by protein localization. The possibility of differential TRPM8 localization in both plasma membrane and ER membrane depending on cell type may be a distinctive feature of this TRP member. Taking into account that the 95 kDa protein displayed a stronger expression than the expected 125 kDa protein in the LNCaP cell line, we hypothesize that such a discrepancy in both expression pattern and amount of each putative isoforms might explain the loss of TRPM8 channel in the plasma membrane.

Possible physiological roles of TRPM8 in the prostate – The role of TRPM8 cold receptor in prostate epithelial cells is not yet clear, but as it is due to their physiology, it is most likely to be related to such processes as proliferation (33, 34), apoptosis (17, 18, 35), differentiation (35, 36) or secretion. The extent of TRPM8 involvement in each of these processes may be determined by preferential subcellular localization of the protein.

Since the prostate is not subjected to any essential temperature variations, the existence of an alternative to cold endogenous agonist(s) involved in TRPM8 activation is quite likely. Indeed, other temperature-sensitive members of the TRP family have previously been shown to be potentially activated by such stimuli as anandamide and PIP_2 for TRPV1 (37), or anandamide, arachidonic acid and phorbol esters for TRPV4 (38, 39). Moreover, the possibility of functional control of TRPM8 by PIP_2 has recently been demonstrated (40). Since an application of exogenous PIP_2 was able to activate TRPM8 as well as to prevent a rundown of the menthol-activated current, it was suggested that the PIP_2 level may be an important regulator of cold transduction *in vivo*. However, due to the lack of evidence proving the involvement of temperature in the prostate function, further investigations are still needed to establish alternative TRPM8 activation pathway(s) in the prostate.

Our results show that TRPM8 represents an important route for intracellular Ca^{2+} store depletion. Store depletion has previously been shown to be critical in promoting growth arrest and apoptosis of prostate cancer epithelial cells (17, 18, 33, 41). Reduced basal filling of intracellular Ca^{2+} stores is also the hallmark of androgen-independent, apoptosis-resistant cell phenotypes characteristic of advanced prostate cancer (18, 35, 41). Thus, as a molecular entity capable of influencing ER Ca^{2+} store filling and promoting Ca^{2+} influx, TRPM8 may be considered as an important determinant in controlling the apoptotic status of prostate cancer epithelial cells and as such, as a potential target for therapeutic interventions. In fact, the involvement of TRPM8 in LNCaP cells apoptosis has recently been suggested (26). However, these authors suggested that TRPM8 acts as a Ca^{2+} permeable channel in both ER and PM membrane, and that menthol-induced cell death is mediated at least in part by the sustained increase in $[Ca^{2+}]_c$. Considering our previous data on the prevalent role of ER store depletion over Ca^{2+} entry in promoting androgen-dependent LNCaP cell death (17), we believe that the primary reason for menthol-induced apoptosis might be store-depletion via ER localized TRPM8. More interstingly, these authors demonstrated that the siRNA targeted against TRPM8 (down-regulating TRPM8 protein expression by ~ 50%) drastically decreased the percentage (by about 40%) of viable LNCaP cells. These results suggest that the endogenous ER TRPM8 activity promotes cell survival by regulating the ER Ca^{2+} store content and/or I_{SOC} activity. This hypothesis is heightened by the fact that i) the *trpm8* expression and the ER TRPM8 activity are both tightly regulated by androgens and ii) the *trpm8* gene is overexpressed in androgen-dependent prostate cancer characterized by an increased cell viability (26, 31).

Given the importance of androgens in the regulation of the proliferative and apoptotic activity of prostate cancer cells, it is imperative to establish how these processes involve TRPM8.

REFERENCES

1. Clapham, D.E., Runnels, L.W., and Strubing, C. (2001) *Nat. Rev. Neurosci.* **2,** 387-396.
2. Montell, C., Birnbaumer, L., and Flockerzi, V. (2002) *Cell* **108,** 595-598.
3. Minke, B., and Cook, B. (2002) *Physiol. Rev.* **82,** 429-472
4. Clapham, D.E. (2003) *Nature* **426,** 517-524
5. Moran, M.M, Xu, H., and Clapham, D.E. (2004) *Curr. Opin. Neurobiol.* **14,** 362-369
6. Gunthorpe, M.J., Benham, C.D., Randall, A., and Davis, J.B. (2002) *Trends Pharmacol. Sci.* **23,** 183-191
7. Peier, A.M., Reeve, A.J., Andersson, D.A., Moqrich, A., Earley, T.J., Hergarden, A.C., Story, G.M., Colley, S., Hogenesch, J.B., McIntyre, P., Bevan, S., and Patapoutian, A. (2002) *Science* **296,** 2046-2049
8. Smith, G.D., Gunthorpe, M.J., Kelsell, R.E., Hayes, P.D., Reilly, P., Facer, P., Wright, J.E., Jerman, J.C., Walhin, J.P., Ooi, L., Egerton, J., Charles, K.J., Smart, D., Randall, A..D., Anand, P., and Davis, J.B. (2002) *Nature* **418,** 186-190
9. Xu, H., Ramsey, I.S., Kotecha, S.A., Moran, M.M., Chong, J.A., Lawson, D., Ge, P., Lilly, J., Silos-Santiago, I., Xie, Y., DiStefano, P.S., Curtis, R., and Clapham, D.E. (2002) *Nature* **418,** 181-186
10. Caterina, M.J., Schumacher, M.A., Tominaga, M., Rosen, T.A., Levine, J.D., and Julius, D. (1997) *Nature* **389,** 816-824
11. Caterina, M.J., and Julius, D. (1999) *Curr Opin Neurobiol* **9,** 525-530
12. McKemy, D.D., Neuhausser, W.M., and Julius, D. (2002) *Nature* **416,** 52-58
13. Peier, A.M., Moqrich, A., Hergarden, A.C., Reeve, A.J., Andersson, D.A., Story, G.M., Earley, T.J., Dragoni, I., McIntyre, P., Bevan, S., and Patapoutian, A. (2002) *Cell* **108,** 705-715
14. Story, G.M., Peier, A.M., Reeve, A.J., Eid, S.R., Mosbacher, J., Hricik, T.R., Earley, T.J., Hergarden, A.C., Andersson, D.A., Hwang, S.W., McIntyre, P., Jegla, T., Bevan, S., and Patapoutian, A. (2003) *Cell* **112,** 819-829
15. Tsavaler, L., Shapero, M.H., Morkowski, S., and Laus, R. (2001) *Cancer Res.* **61,** 3760-3769
16. Horoszewicz, J.S., Leong, S.S., Kawinski, E., Karr, J.P., Rosenthal, H., Chu, T.M., Mirand, E.A., and Murphy, G.P. (1983) *Cancer Res.* **43,** 1809-1818
17. Skryma, R., Mariot, P., Bourhis, X.L., Coppenolle, F.V., Shuba, Y., Vanden Abeele, F., Legrand, G., Humez, S., Boilly, B., and Prevarskaya, N. (2000) *J. Physiol.* **527,** 71-83
18. Vanden Abeele, F., Skryma, R., Shuba, Y., Van Coppenolle, F., Slomianny, C., Roudbaraki, M., Mauroy, B., Wuytack, F., and Prevarskaya, N. (2002) *Cancer Cell.* **1,** 169-179
19. Vanden Abeele, F., Roudbaraki, M., Shuba, Y., Skryma, R., and Prevarskaya, N. (2003) *J. Biol. Chem.* **278,** 15381-15389
20 Vanden Abeele F., Shuba, Y., Roudbaraki, M., Lemonnier, L., Vanoverberghe, K., Mariot, P., Skryma, R., and Prevarskaya N. (2003) *Cell Calcium* **33,** 357-373
21. Vanden Abeele, F., Lemonnier, L., Thebault, S., Lepage, G., Parys, J.B., Shuba, Y., Skryma, R., and Prevarskaya, N. (2004) *J. Biol. Chem.* **279,** 30326-30337
22. Brooks, S.P., and Storey, K.B. (1992) *Anal. Biochem.* **201,** 119-126
23. Chomczynski, P., and Sacchi, N. (1987) *Anal. Biochem.* **162,** 156-159
24. Manders, E.M.M., Verbeek, F.J., and Alen, J.A. (1993) *J. Microsc.* **169,** 375-382
25. Grynkiewicz, G., Poenie, M., and Tsien, R.Y. (1985) *J. Biol. Chem.* **260,** 3440-3450.
26. Zhang, L., and Barritt, G.J. (2004) *Cancer Res.* **64,** 8365-8373
27. Skryma, R.N., Prevarskaya, N.B., Dufy-Barbe, L., Odessa, M.F., Audin, J., and Dufy, B. (1997) *Prostate* **33,** 112-122
28. Skryma, R., Van Coppenolle, F., Dufy-Barbe, L., Dufy, B., and Prevarskaya, N. (1999) *Receptors Channels* **6,** 241-253
29. Bavari, S., Bosio, C.M., Wiegand, E., Ruthel, G., Will, A.B., Geisbert, T.W., Hevey, M., Schmaljohn,

C., Schmaljohn, A., and Aman, M.J. (2003) *J. Exp. Med.* **195,** 593-602
30. Naal, R.M., Holowka, E.P., Baird, B., and Holowka, D. (2003) *Traffic* **4,** 190-200
31. Bidaux, G., Roudbaraki, M., Merle, C., Crepin, A., Delcourt, P., Slomiany, C., Thebault, S., Bonnal, J.L., Benahmed, M., Cabon, F., Mauroy, B., and Prevarskaya, N. (2005) *Endocr. Relat. Cancer*, **12**(2):367-382
32. Tsuzuki, K., Xing, H., Ling, J., and Gu, J.G. (2004) *J. Neurosci.* **24,** 762-771
33. Vanoverberghe, K., Mariot, P., Vanden Abeele, F., Delcourt, P., Parys, J. B., and Prevarskaya, N. (2003) *Cell Calcium* **34,** 75-85
34. Thebault, S., Roudbaraki, M., Sydorenko, V., Shuba, Y., Lemonnier, L., Slomianny, C., Dewailly, E., Bonnal, J.L., Mauroy, B., Skryma, R., and Prevarskaya, N. (2003) *J. Clin. Invest.* **111,** 1691-1701
35. Vanoverberghe, K., Vanden Abeele, F., Mariot, P., Lepage, G., Roudbaraki, M., Bonnal, J.L., Mauroy, B., Shuba, Y., Skryma, R., and Prevarskaya, N. (2004) *Cell Death Differ.* **11,** 321-330
36. Mariot, P., Vanoverberghe, K., Lalevee, N., Rossier, M.F., and Prevarskaya, N. (2002) Overexpression of an alpha 1H (Cav3.2) *J. Biol. Chem.* **277,** 10824-10833
37. Prescott, E.D., and Julius, D. (2003) *Science* **300,** 1284-1288
38. Watanabe, H., Vriens, J., Prenen, J., Droogmans, G., Voets, T., and Nilius, B. (2003) *Nature* **424,** 434-438
39. Gao, X., Wu, L., and O'Neil, R.G. (2003) *J. Biol. Chem.* **278,** 27129-27137
40. Liu, B., and Qin, F. (2005) *J. Neurosci.* **25,** 1674-1681
41. Prevarskaya, N., Skryma, R., and Shuba, Y. (2004) *Biochem. Biophys. Res. Commun.* **322,** 1326-1235

FOOTNOTES

*This work was supported by grants from INSERM, the Ministère de l'Education, La Ligue Nationale Contre le Cancer, l'ARC, the region Nord/Pas-de-Calais.
‡Supported by the Ministère de l'Education (France).
[1]Department of Basic Medical Sciences, Pharmacology, St. George's Hospital Medical School, Cranmer Terrace, London SW17 0RE, UK. D. Gordienko was supported by the Welcome Trust (062926,075112).
[2]Institute for Information Transmission Problems, RAS, Bolshoi Karetny pereulok 19, Moscow 101447, and A. N. Belozersky Institute, Moscow State University, Moscow 119899, Russia

[3]Permanent address: Bogomoletz Institute of Physiology, NASU, Bogomoletz Street, 4, 01024 Kiev, Ukraine.
†Contributed equally to this work.
¶Share senior authorship.

[1]The abbreviations used are: $[Ca^{2+}]_c$, cytosolic calcium concentration; $[Ca^{2+}]_{out}$, extracellular calcium concentration; NPE, normal prostate epithelial cells; BPHE, benign prostate hyperplasia epithelial cells; TRPM8, human transient receptor potential melastatine 8; ER, endoplasmic reticulum; LNCaP, lymph node carcinoma of the prostate; HEK-293, human embryonic kidney 293; SOCE, store-operated calcium entry; PM, plasma membrane; HBSS, Hank's balanced salt solution.

FIGURE LEGENDS

Fig. 1. Expression of TRPM8 in prostatic cell lines. **A:** Agarose gel showing the expression of TRPM8 mRNA in LNCaP cells and lack thereof in DU-145, PC-3 and PNT1A prostatic cell lines as well as in HEK-293 cells, as determined by RT-PCR. **B:** Agarose gel showing the expression of the TRPM8 mRNA in pEGFP-TRPM8-transfected HEK-293 cells, but neither in HEK-293/wt (wild-type), nor in empty vector-transfected HEK-293/pEGFP cells. 1 kb DNA ladder (M (bp)) was used as DNA size marker in both experiments. See Methods for details.

Fig. 2. LNCaP cells do not show a "classical" menthol-activated, TRPM8-mediated current due to lack of TRPM8 localization in the plasma membrane. **A:** Averaged time courses of membrane current development (measured at +100 mV, mean±s.e.m) in the control (HEK-293/pEGFP, filled circles, n=4) and TRPM8-expressing (HEK-293/pEGFP-TRPM8, open circles, n=6) HEK-293 cells during exposure to menthol (100 μM, marked by horizontal bar). The inset shows the representative I-V relationship of steady-state menthol-activated current in TRPM8-expressing cells. **B:** Averaged I-V relationships of membrane current in LNCaP cells under normal ionic conditions from both sides of the membrane (mean±s.e.m) before (ctrl., circles, n=6) and after exposure to menthol (100 μM, triangles, n=6); inset represents respective I-Vs from a representative cell at amplified current density scale showing the appearance of some small inward current in the presence of menthol. **C:** Representative confocal images of HEK-293 (left panel) and LNCaP (right panel) cells heterologously expressing GFP-tagged TRPM8. Whilst in HEK-293 cells clear clusters of GFP fluorescence are visible on the perimeter of the cells, which corresponds to plasma membrane localization of TRPM8-GFP construct, in LNCaP cells GFP fluorescence corresponds to intracellular-restricted areas only. **D:** Separately collected confocal images of LNCaP cells double-labeled with anti-TRPM8 antibody (visualized with Alexa546-labeled secondary antibody, left panel) and plasma membrane marker, FITC-conjugated Cholera Toxin subunit B (CTB, middle panel). The right panel represents an overlay of the two images with blown-up selected plasma membrane region (6.66-fold numerical magnification) showing an absence of co-localization between TRPM8 and CTB. The bright blue line on the blown-up image defines a region of interest (ROI), for which a co-localization coefficient was determined (see text for details).

Fig. 3. Electrophysiological properties of cold/menthol-activated membrane current in LNCaP cells. **A:** Averaged time course of inward current activation (measured at –100 mV, mean±s.e.m., n=6) in response to cooling in LNCaP cells. The temperature of Na^+-, K^+-free, 10 mM Ca^{2+}-containing bath solution was reduced from 37°C to 22°C at time 0 (depicted by horizontal bars on the top). The inset shows representative I-V relationship of maximally developed current in response to cooling acquired with ±100 mV voltage ramp. **B:** Same as in **A**, but in response to menthol (100 μM, marked on top by horizontal bar) applied at 36°C (n=5). **C:** Representative I-V relationships of menthol-activated current in the presence of Ca^{2+}, Sr^{2+} or Na^+ as a charge carrier. Inset shows quantification of the selectivity properties of the channels activated by menthol in LNCaP cells based on maximal currents (measured at –100 mV), carried by specified ions relative to Ca^{2+} current (mean±s.e.m., n=4-6 for each ion substitutions). **D:** Summary of the inhibitory effects (mean±s.e.m.) of flufenamate (10 μM, n=5), SK&F 96365 (50 μM, n=6) and ruthenium red (10 μM, n=4) on menthol-activated current in LNCaP cells.

Fig. 4. TRPM8 knock-down eliminates functional responses to menthol in LNCaP cells. **A:** Three left columns: Western blots with anti-TRPM8 antibody showing disappearance of TRPM8 protein-specific bands in TRPM8 antisense (AS) vs. sense ODNs-treated (for 48 hours) LNCaP cells as well as LNCaP cells transfected with $siRNA_{TRPM8}$ (see also legend to panel D); two right columns: Western blots with anti-TRPM8 antibody showing the presence of TRPM8 protein-specific bands in HEK-293/TRPM8 cells and lack thereof in HEK-293/ctrl cells. **B:** Averaged time courses of inward current (measured at –100 mV, mean±s.e.m.) activation in response to menthol in LNCaP cells treated with sense (n=6, circles, control) and antisense (n=8, triangles) ODNs; menthol was applied at time "0". **C:** Averaged time courses

of $[Ca^{2+}]_c$ changes (measured as F_{340}/F_{380} ratio, mean±s.e.m.) during menthol application in Ca^{2+}-free (0/Ca) and Ca^{2+}-containing (2/Ca) bath solution in TRPM8 sense (n=64, open circles, control) and antisense (n=72, filled circles) ODNs-treated LNCaP cells. **D:** RT-PCR assay on the changes of TRPM8 mRNA on 2nd, 4th and 7th day following transfection of LNCaP cells with 100 nM of $siRNA_{TRPM8}$ (upper panel); cells treated with vehicle alone (Ctrl) served as control. Lower panel – representative confocal images of LNCaP cells stained with anti-TRPM8 antibody 2 days after vehicle treatment (left image) or transfection with 100 nM $siRNA_{TRPM8}$ (right image). **E:** Averaged time courses of inward current (measured at –100 mV, mean±s.e.m.) activation in response to menthol in LNCaP cells 2 days after vehicle treatment (open circles, n=5) or transfection with $siRNA_{TRPM8}$ (filled circles, n=8). **C:** Averaged time courses of $[Ca^{2+}]_c$ changes (measured as F_{340}/F_{380} ratio, mean±s.e.m.) during menthol application in Ca^{2+}-free (0/Ca) and Ca^{2+}-containing (2/Ca) bath solution in LNCaP cells 2 days after vehicle treatment (open circles, n=27) or transfection with $siRNA_{TRPM8}$ (filled circles, n=30).

Fig. 5. Menthol induces TRPM8-mediated ER Ca^{2+} store depletion in LNCaP cells. **A:** The average time course of relative $[Ca^{2+}]_{ER}$ reduction (mean±s.e.m., n=28) in response to successive application of menthol (100 μM) and ionomycine (IM, 1 μM) measured using Mag-Fluo 4 on digitonin-permeabilized LNCaP cells. Insets show representative images taken at points indicated by arrows. **B:** Same as in **A**, but in response to two successive menthol (100 μM) applications, the second of which was made in the presence of IP_3-R and RyR blockers heparin (500 μg/ml) and ryanodine (20 μM), respectively. **C:** Same as in **A**, but acquired in LNCaP cells treated for 72 hours with TRPM8-specific sense (filled circles, n=12) and antisense (open circles, n=11) ODNs.

Fig. 6. Icilin-induced Ca^{2+} release does not involve IP_3 or ryanodine receptors activation. **A, B, C:** Representative confocal images (taken at 1/s frame rate, frame numbers are indicated in the images, left panels) and time courses (right panels) of icilin-induced Ca^{2+} release in fluo-3AM-loaded LNCaP cells in 2 mM Ca^{2+}-containing (**A, C**) and Ca^{2+}-free (**B**) extracellular medium. Exposure of the cell to the SERCA pump inhibitor, cyclopiazonic acid (CPA, 20 μM), did not produce additional $[Ca^{2+}]_{in}$ increase following icilin application (**A**), suggesting nearly complete store depletion by icilin, whilst IP_3 and ryanodine receptor blockers, xestospongin C and ryanodine, respectively, did not prevent icilin-induced $[Ca^{2+}]_{in}$ increase, suggesting TRPM8, but not any IP_3-R or RyR involvement.

Fig. 7. Thapsigargin, but not IP_3 interferes with store-dependent current activation by menthol in LNCaP cells. **A:** Representative time course of successive development of two different store-dependent currents (measured at –100 mV) in LNCaP cell – one in response to IP_3 (100 μM) dialysis ($I_{SOC/CC}$) and another one in response to menthol (100 μM) application ($I_{SOC/menthol}$); time "0" corresponds to the establishing whole-cell configuration with IP_3-containing pipette; similar experiment was repeated 5 times. **B:** Averaged time courses of $I_{SOC/menthol}$ (measured at –100 mV, mean±s.e.m.) activation in control LNCaP cells (circles, n=5) and cells pre-incubated with thasigargin (TG, 0.1 μM, triangles, n=8).

Fig. 8. Expression of TRPM8 and $I_{SOC/menthol}$ are androgen dependent. **A:** Normalized changes of TRPM8 mRNA assayed by semi-quantitative RT-PCR in LNCaP cells cultured under steroid-deprived conditions (light grey columns) and following addition of 5α-dihydrotestosterone (DHT, 10^{-9} M, dark grey columns); TRPM8 mRNA level in LNCaP cells just before steroid deprivation was taken to be 100%; mean±s.e.m. n=4. Culturing conditions are marked by horizontal bars. **B:** Averaged time courses of $I_{SOC/menthol}$ (measured at –100 mV, mean±s.e.m.) activation in control LNCaP cells (open circles, n=5), cells cultured for 96 h under steroid deprived conditions (square, n=8), and following addition of 5α-dihydrotestosterone (DHT, 10^{-9} M, black circles, n=12). **C:** Averaged time courses of $[Ca^{2+}]_c$ changes (measured as F_{340}/F_{380} ratio, mean±s.e.m.) during menthol application in Ca^{2+}-free (0/Ca) and Ca^{2+}-containing (2/Ca) bath solution in control LNCaP cells (black circles, n=72) and in cells cultured for 96 h under steroid deprived conditions (open circles, n=104)).

TABLES

Table 1. Single nucleotide polymorphism (SNP) comparison of different TRPM8 ORF with the TRPM8 sequence cloned from LNCaP cells.

Clones	SNP at position 173		SNP at position 2383	
	Nucleotide	Amino acid	Nucleotide	Amino acid
AY328400 (Prostate tissue)	C	T	G	A
DQ139309 (LNCaP)	C	T	A	T
NM_024080	T	I	A	T
AY090109	T	I	A	T
AB061779	C	T	A	T
NT_005120.14	C	T	A	T
EST: BE390627.1	C	T	-	-
EST: BE274448.1	C	T	-	-
Mouse (NP_599013)	C	T	A	T
Rat (NP_599198)	C	T	A	T
Consensus	C	T	A	T

Figure 1

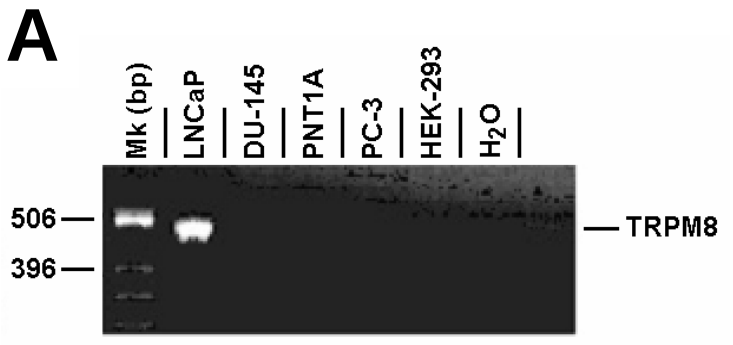

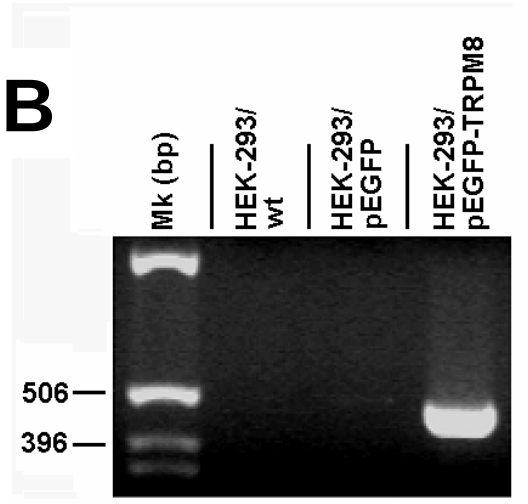

Figure 2

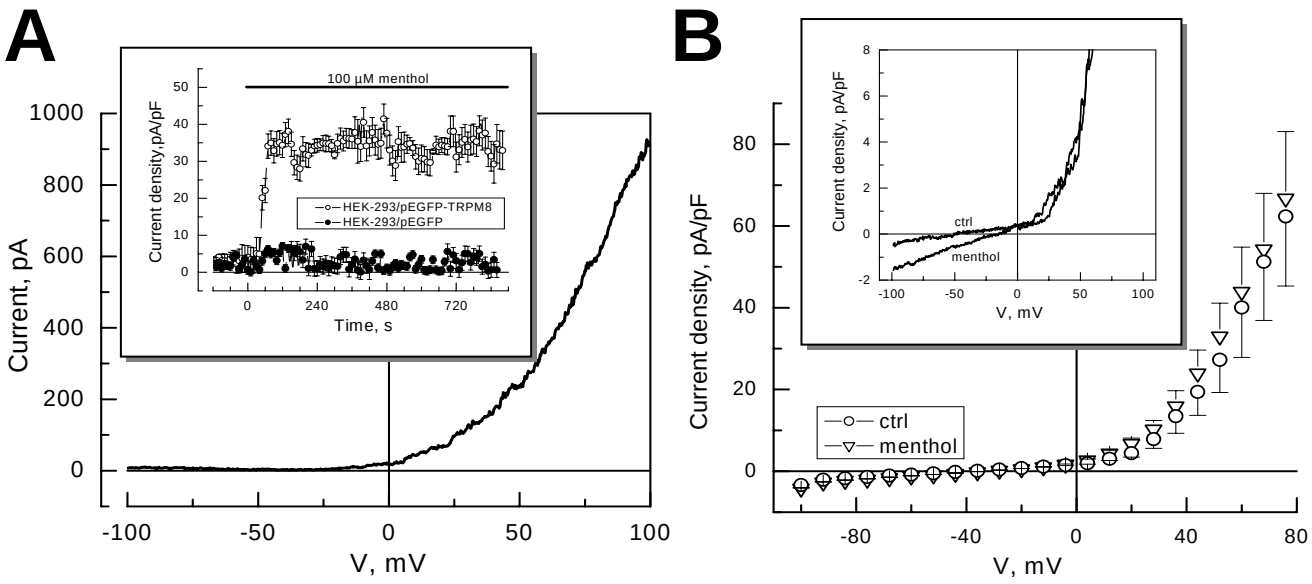

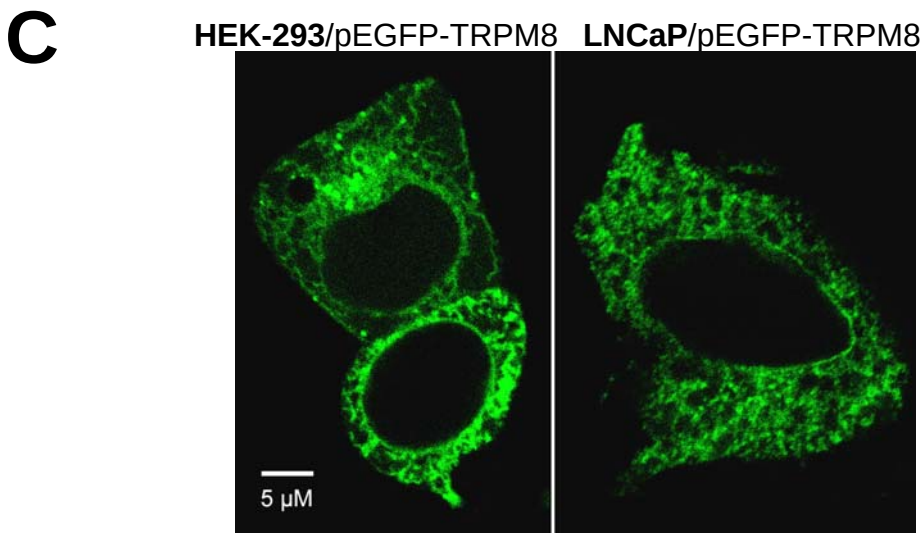

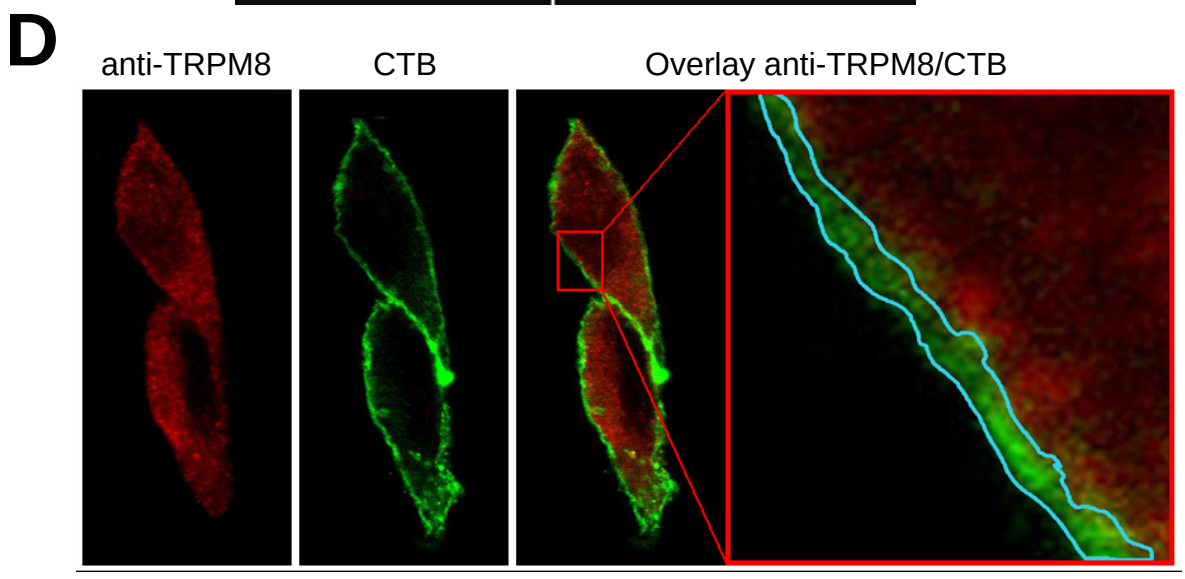

Figure 3

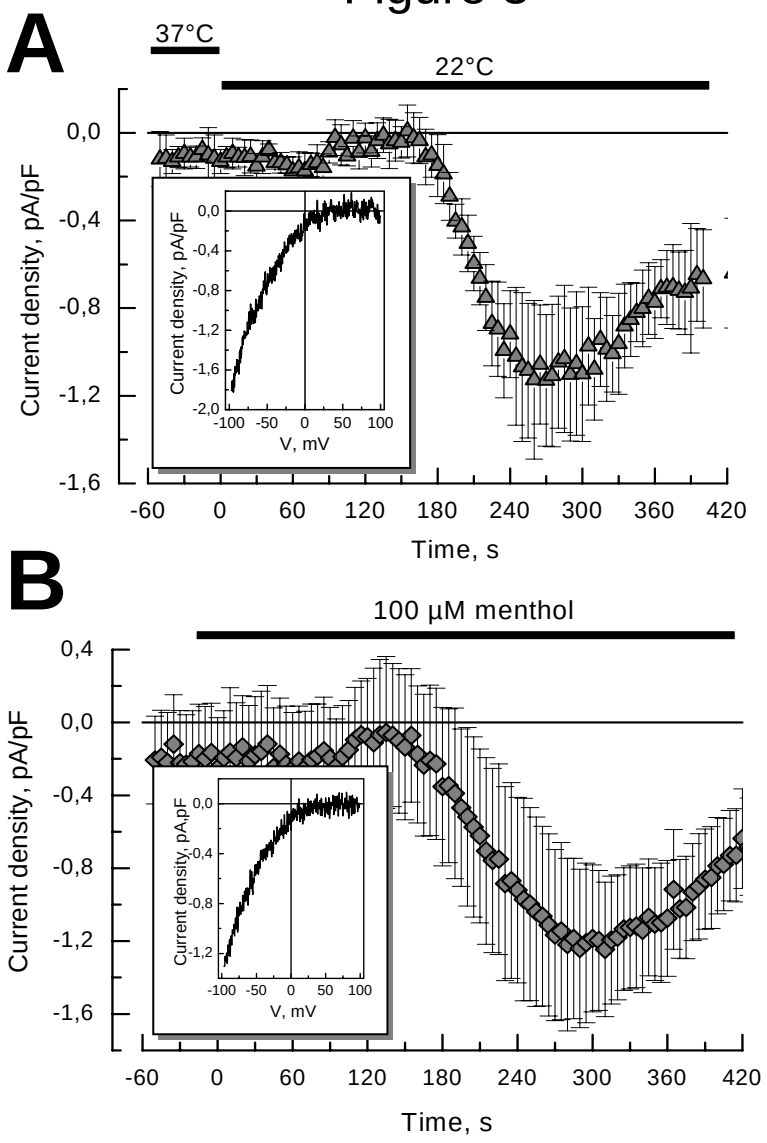

Figure 4

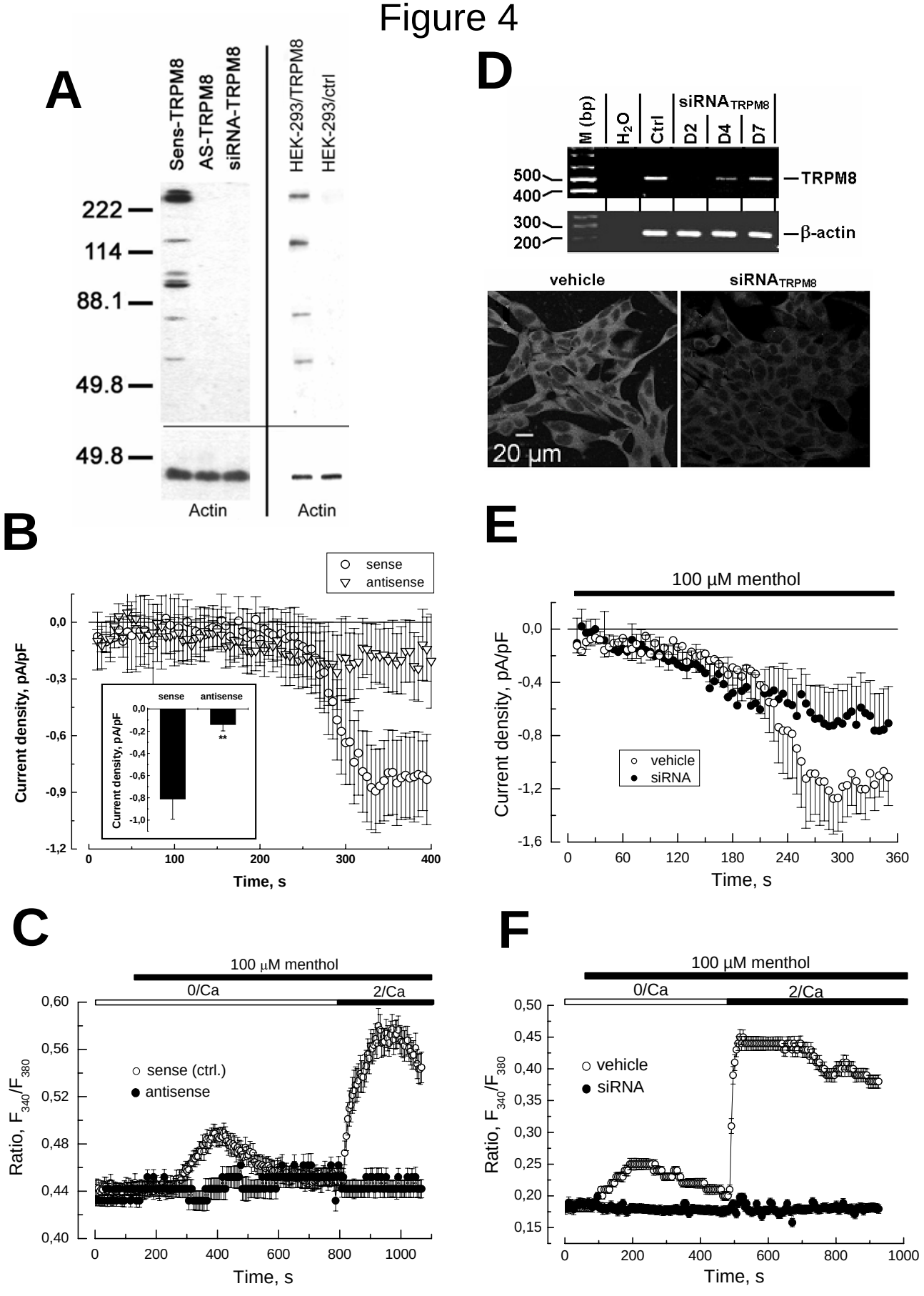

Figure 5

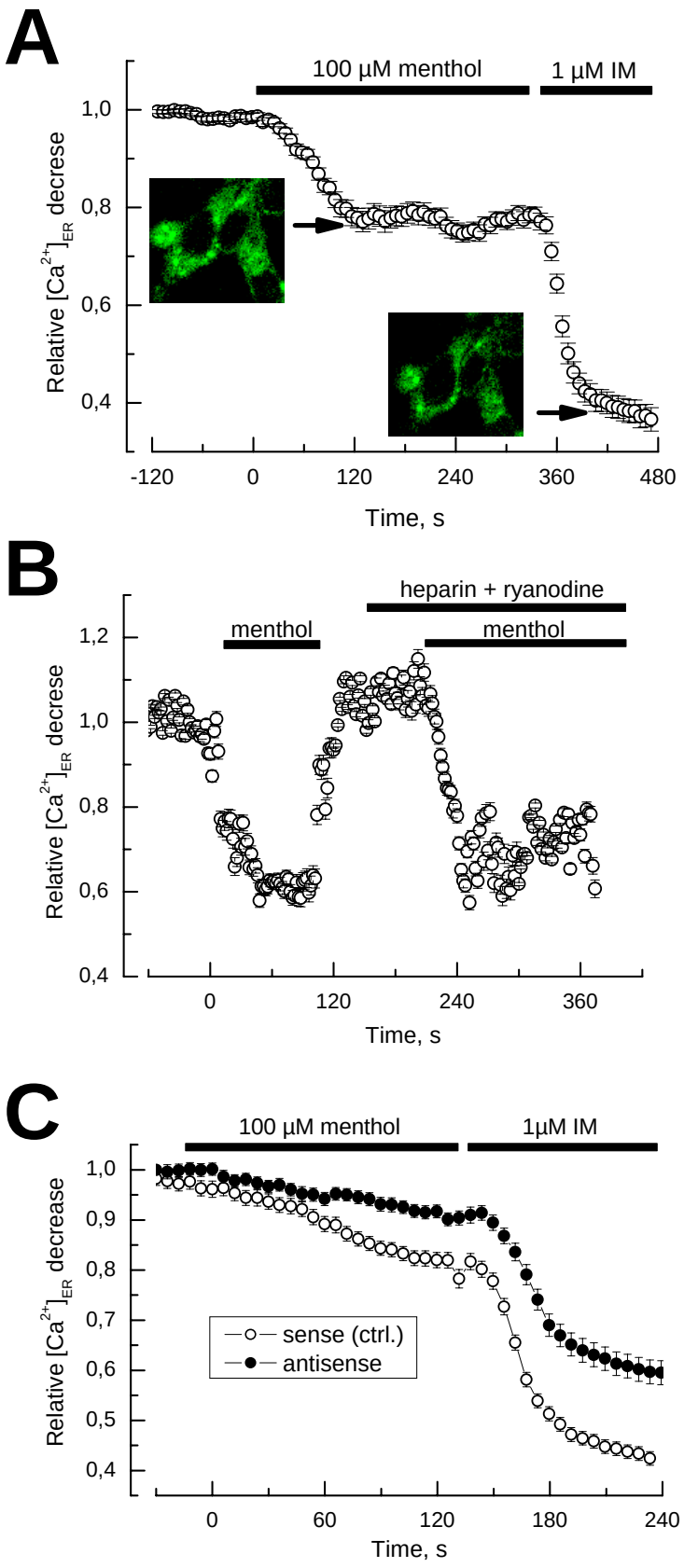

Figure 6

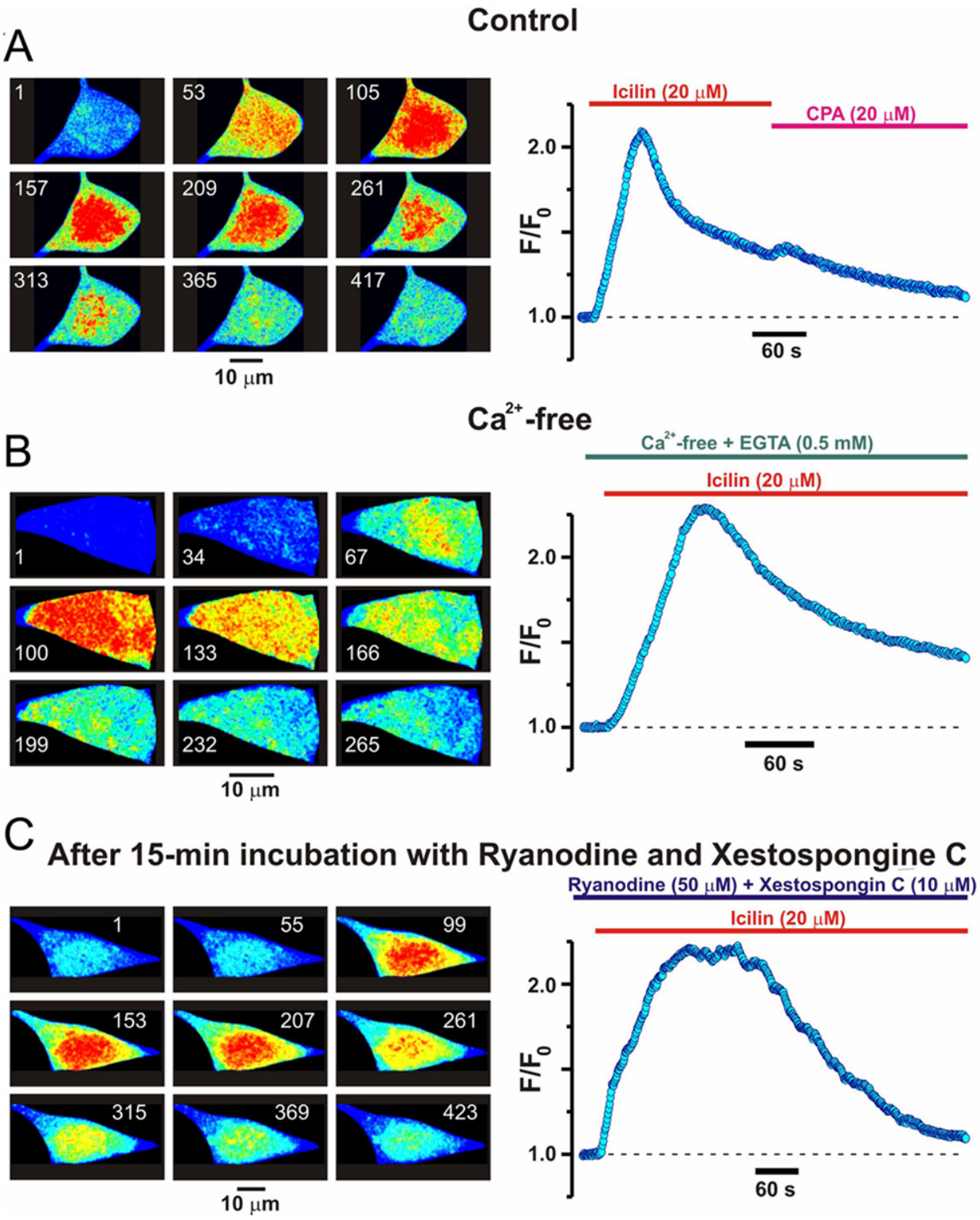

Figure 7

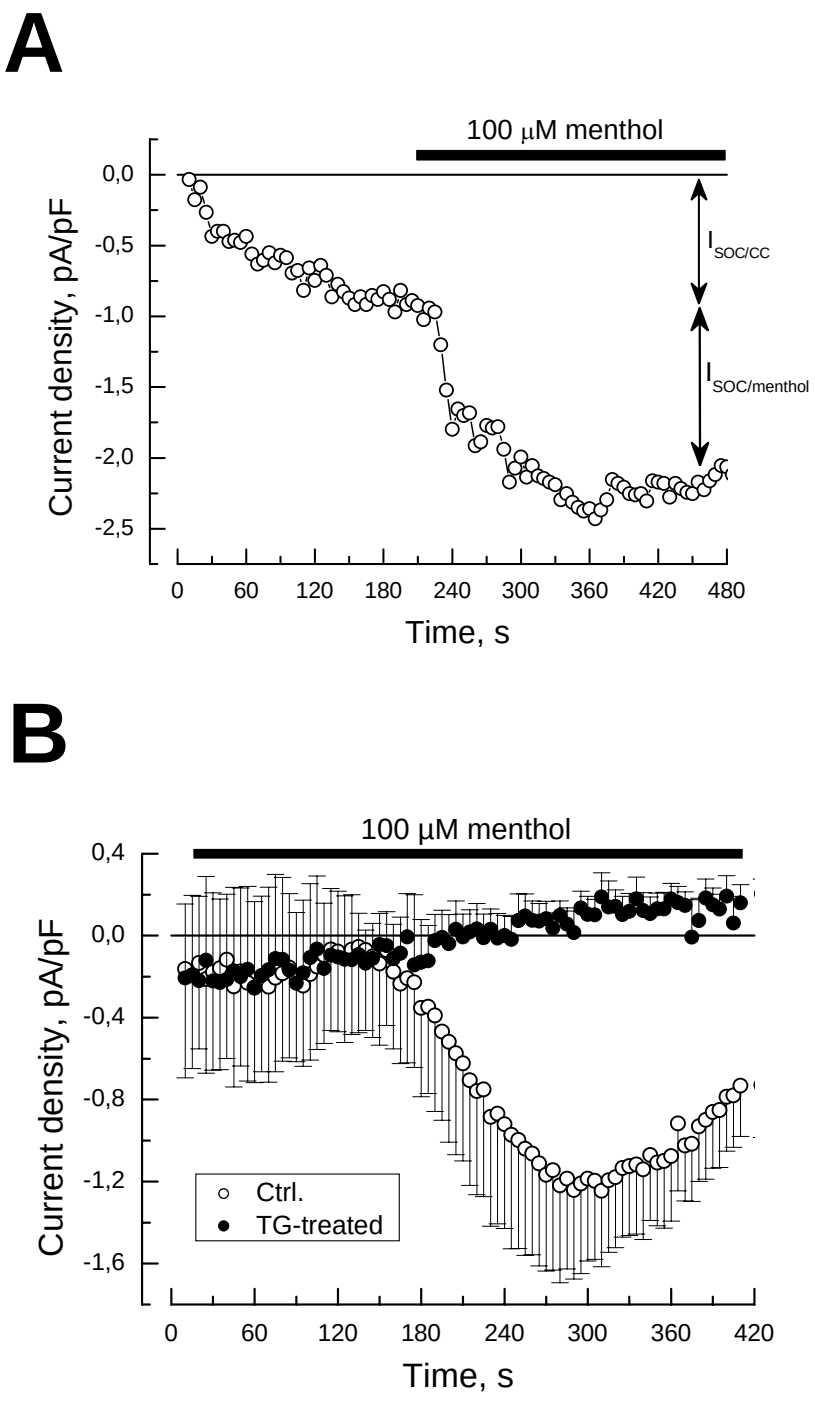

Figure 8